Punjab University Journal of Mathematics (2026), 58(02), 155- 186
https://doi.org/10.52280/pujm.2026.58(02)01

Mathematical and Numerical Analysis of COVID-19 Epidemic Model with Vaccination and Treatment

Received
02 March, 2026

Revised
24 March, 2026
13 April, 2026

Accepted
20 April, 2026

Published Online
29 July, 2026

Raed Hameed Mahdi[a], *Shah Zeb[b]
[a]School of Mathematical Sciences,
Universiti Sains Malaysia, Penang, Malaysia

[b]School of Distance Education,
Universiti Sains Malaysia, Penang, Malaysia

Ayesha Kamran
Department of Mathematics,
University of Management and Technology, Lahore, Pakistan

Muhammad Rafiq
Department of Mathematics,
Namal University, Mianwali, Pakistan

Yasir Nawaz
Department of Basic Sciences,
The Superior University, Lahore, Pakistan

Muhammad Bilal, Muhammad Irfan
Department of Mathematics,
University of Layyah, Layyah, Pakistan

Abstract. Mathematical modeling is a broad field that greatly impacts and contributes to collaborative research investigations. The models Improve research on the fundamental the quantitative attitude and dynamics of diseases that are infectious that harm humans, including COVID-19, human immunodeficiency virus (HIV), and hepatitis B virus. This paper introduces a framework that supports the analysis of COVID-19 using an epidemic model that incorporates vaccination and treatment. The framework enables the examination of both non-pharmaceutical interventions and pharmaceutical interventions. The preservation of the basic reproduction number ensures the standardization of the stability of disease-free (DFE) and endemic equilibria. The local stability of the endemic and disease-free equilibria is proven using the Routh-Hurwitz criterion. The demonstration of disease-free and endemic equilibria convergence

*Corresponding Author :shahzeb@student.usm.my

and divergence is demonstrated through the utilization of Standard and non-standard finite differences (SFD and NSFD, respectively) techniques. It might be argued that SFD schemes, specifically Runge-Kutta order four (RK-4) and Euler schemes, demonstrate convergence at smaller step sizes. However, the NSFD scheme is intended to enhance understanding of the dynamic behavior of the continuous model. Empirical evidence demonstrates that the NSFD technique converges, irrespective of the chosen step size. The latter refers to a powerful, effective, and dependable technique that provides a clear representation of the continuous model. Numerical simulations are employed to validate all the data, enhancing our understanding of the causes of the illness. The theoretical and quantitative results of its study can serve a valuable for mechanism tracking the transmission as to COVID-19.

AMS (MOS) Subject Classification Codes: 92D30; 34K20; 92D25
Key Words: Mathematical modeling, local stability, Epidemic model, Numerical scheme.

1. INTRODUCTION

Infectious diseases arise from a dynamic interaction between a pathogenic microorganism (such as bacteria, fungi, parasites, or viruses, including prions) and a host organism. It is emphasized that antimicrobial drugs and vaccinations can effectively cure and eradicate many infectious diseases, while also being able to prevent them through the use of suitable antibiotics, hygiene practices, and preventive measures. However, due to the natural evolution of infectious organisms that resist treatment medications, as well as the ongoing social and environmental changes caused by globalization and urbanization, these organisms also show significant unpredictability in terms of their impact on the population's health. The study of infectious disease dynamics has had significant growth over the past 70 years, evolving into a comprehensive multidisciplinary field that integrates epidemiology, public health, and other related disciplines [13, 36, 44]. The current global outbreak of coronavirus disease 2019 (COVID-19) is a significant concern in the field of social medicine. The pathogen responsible for the COVID-19 disease is referred to as SARS-CoV-2, which stands for severe acute respiratory syndrome coronavirus-2 [1, 3, 5, 9, 44, 45]. The initial instance of this novel coronavirus, often manifesting as pneumonia, was detected in Wuhan, China in December 2019 [4, 9, 11]. The rapidity with which this disease spreads among individuals is one of its most lethal traits. COVID-19 is transmitted between individuals through two distinct pathways: direct contact with contaminated surfaces and the inhalation of respiratory droplet emitted by infected peoples. Following exposure to virus, COVID-19 typically incubates for a period of two to fourteen days. Some of the most prevalent analytical symptoms of COVID-19 are fever, dry cough, dyspnea, and fatigue [46, 30, 8]. The outbreak was officially declared a pandemic by the World Health Organization (WHO) on March 11, 2020, following its initial classification as a Public Health Emergency of International Concern in January 2020 [21, 35]. As of March 7th, 2021, there were more than 116.17 million confirmed cases and almost 2.58 million documented deaths [47]. The WHO report on COVID-19, as of August 10, 2021, states that more 202.14 million people

have been infected with virus and over 4.28 million have died from it. The global outbreak of COVID-19, caused by the novel coronavirus SARS-CoV-2, has posed unprecedented challenges to public health systems and economic worldwide since its emergence in Wuhan in late 2019 [37]. Characterized by rapid human to human transmission through respiratory droplets and the presence of asymptomatic carriers, the disease exhibits complex dynamics that complicate its control and prediction [21]. These features make COVID-19 particularly suitable for investigation through mathematical modeling, where compartmental frameworks such as the SIR model and its extensions are employed to describe the spread of infection within a population [25]. Such models enable the estimation of key epidemiology parameters, including transmission and recovery rate, and provide insights into the impact of intervention strategies like quarantine, social distancing, and vaccination. Consequently, mathematical modeling serves as an essential tool for understanding the transmission behavior of COVID-19 and for supporting evidence-based decision-making in controlling the pandemic [12, 42].

The study of mathematical modeling of infectious diseases has gained significant attention due to the occurrence of consecutive epidemics, including HIV in the 1980s which is still prevalent [15, 16, 17, 24], the SARS epidemic in 2002-2003 [2, 7, 14, 20], H5N1 influenza in 2005 [27, 6], H1N1 in 2009 [26, 19], and Ebola in 2014 [16, 15]. The COVID-19 pandemic has prompted unprecedented efforts in mathematical modeling within the field of epidemiology. A multitude of mathematical methodologies have been developed to examine epidemiological matters. However, the primary emphasis in epidemiological mathematical modeling remains on appropriately simple and validated models. The pioneering work of W. O. Kermack and A. G. McKendrick on the SIR model [22, 23, 49], marks the beginning of contemporary study in mathematical epidemiology. This model was inspired by the Spanish flu pandemic that occurred from 1918 to 1919 [45,46]. Several advance-ments in modeling have been made, including multi-compartment models [26], models with time-varying or nonlinear disease transmission rates, multi-patch models, multi-group models that consider population heterogeneity, and epidemic models that incorporate vac-cination and other control measures [27-29]. Spatiotemporal models are used to represent the spatial distributions of susceptible and infected individuals, considering the random movement of individuals in the population. A more thorough assessment of the literature can be found in the review articles and monographs [30-32]. The authors in [33] investigate the impact of therapy and vaccination on managing the COVID-19 pandemic with optimal control by mathematical modeling. The present study seeks to examine the health haz-ards posed by COVID-19 on the overall population's well-being, in addition to developing strategies for vaccination and treatment of the virus. Several numerical systems, such as the NSFD scheme, RK-4, and Euler, have been employed to determine the model's char-acteristics and demonstrate its accuracy and ecological viability. The results imply that the previously mentioned schemes offer a comprehensive description in the continuous model. The NSFD scheme is considered a more efficient numerical method compared to classical methods such as the Euler method and the RK-4 method. The main advantage of NSFD approach lies in its ability to preserve essential qualitative properties of the original differ-ential equation, including positivity, stability, and boundedness of the solution [41]. Unlike standard schemes, NSFD uses specially constructed denominator functions and nonlocal approximations, which improve the reliability of numerical results even for larger step

sizes [42,43]. As a result, NSFD often provides more accurate and stable solutions while requiring less restrictive step size conditions than Euler and Rk-4 methods. Therefore, the NSFD scheme is regarded as a more efficient and robust approach for solving nonlinear dynamical system, particularly in applications arising in biology and epidemiology [44]. The current article is classed according to its structure. The COVID-19 sickness model and its associated parameters are elucidated in Sections 2 and 3 investigates the continuous model's formulation of R_0, the system's equilibrium points, and whether these points are stable or not. Section 4 of the continuous model creates SFD schemes (RK-4 and Euler), such as the NSFD scheme. When using greater step sizes, both the Euler and RK-4 schemes fail to accurately capture the important dynamic characteristics of the continuous model. This leads to numerical solutions that deviate from the solutions of the original system, particularly in terms of maintaining solution positivity. However, the NSFD scheme effectively resolves the limitations of the SFD schemes by offering positive responses for all limited step sizes. Moreover, the research demonstrates that the NSFD scheme surpasses the Euler and RK-4 schemes in all aspects and exhibits unconditional convergence. Throughout the entire process, numerical simulations consistently validate the theoretical findings. Section 5 presents a concise review of the entire work, encompassing the main conclusions and providing an overview of the findings.

2. Formulations of Mathematical Model

To build the mathematical framework of COVID-19 vacation and treatment. In this area, we divided the entire population into five sections based on the disease status of each entity: Susceptible Compartments (S), Vaccinated Compartments (V), uninfected cell of body (I), infected cell of body(D), Recovered cell of body (R). Susceptible individuals can become vaccinated at rate ϕ or infected through contact with infected individuals, modeled by the nonlinear incidence $\frac{\beta SI}{\sigma+\eta I}$. Vaccinated individuals have partial protection but may still become infected rate ψ. Infected individuals may recover at rate γ or progress to severe disease D at rate α, from which recovery occurs at rate ω. Natural births and deaths are incorporated via Λ and μ. This framework captures the combined effects of vaccination, infection, treatment, and recovery, providing a basis to analyze disease dynamics, evaluate the reproduction number, and assess intervention strategies.

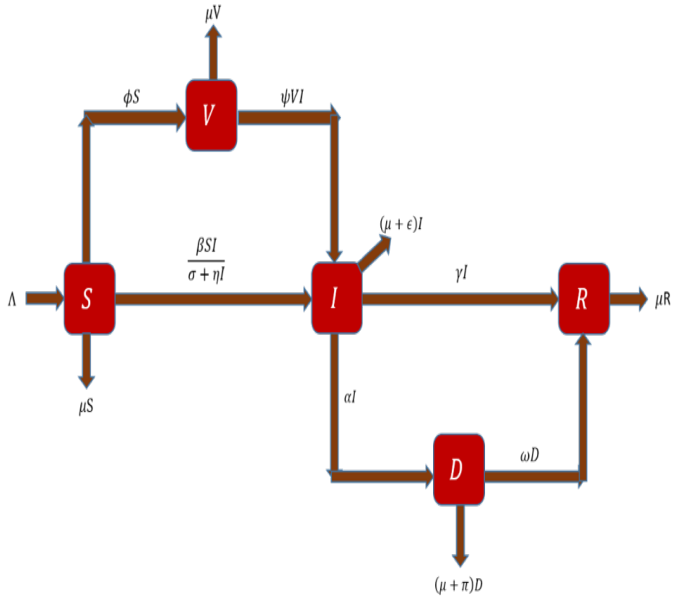

FIGURE 1. $(SLII_sR)$ Model

3. SYSTEM OF MATHEMATICAL MODEL

$$\begin{aligned}
\frac{dS}{dt} &= \Lambda - \frac{\beta SI}{\sigma + \eta I} - \Phi S - \mu S, \\
\frac{dV}{dt} &= \Phi S - (\mu + \psi I)V, \\
\frac{dI}{dt} &= \frac{\beta SI}{\sigma + \eta I} - \psi VI - (\mu + \epsilon + \gamma + \alpha)I, \\
\frac{dD}{dt} &= \alpha I - (\mu + \pi + \omega)D, \\
\frac{dR}{dt} &= \gamma I + \omega D - \mu R.
\end{aligned} \tag{3. 1}$$

3.1. **Parameters.**

$S =$ Show the number susceptible compartments.
$V =$ Shows the number of vaccinated compartments.
$I =$ Show the count of uninfected cells in the body.
$D =$ Show the count of infected cells of body. .
$R =$ Shows the number of recovered cells of body.

Parameter	Value	Description	Ref.
Λ	1.3703	Recruitment rate of susceptibles	Assumed
β	0.0108	Transmission rate	[18]
μ	1	Natural death rate	Assumed
σ	5	Holling saturation constant	[18]
ϕ	0.43	Vaccination rate	Assumed
ψ	0.01	Infection rate of vaccinated individuals	Assumed
ϵ	0.0271	Disease-induced death rate of infected	[18]
η	1	Positive constant	[18]
γ	0.1	Recovery rate of infected	[18]
π	0.4	Disease-induced death rate of quarantined	[18]
α	0.22	Contact rate of non-vaccinated individuals	Assumed
ω	0.2	Recovery rate of quarantined	Assumed

TABLE 1. Parametric Values

4. DISEASE-FREE AND ENDEMIC EQUILIBRIUM POINTS

4.1. **Disease-Free Equilibrium Point.** The disease-free equilibrium (DFE) represents the state in which the disease is absent from the population. It is obtained by setting the infected and disease-related compartments equal to zero, i.e., $I = D = 0$, and equating the right-hand side of model (3.1) to zero. Hence, the disease-free equilibrium point of model (3.1) is given by

$$E_f = (S^*, V^*, I^*, D^*, R^*) = \left(\frac{\Lambda}{\phi+\mu}, \frac{\Lambda\phi}{\mu(\phi+\mu)}, 0, 0, 0\right). \tag{4. 2}$$

4.2. **Endemic Equilibrium Point.** The endemic equilibrium points a positive uniform solution where the disease persists in the population in addition to the DFE. It is found by all the differential equations in model (3.1). first, second, fourth, and fifth equations of system (3.1) should be solved as,

$$\begin{aligned}
S^* &= \frac{\Lambda(\sigma+\eta I^*)}{\beta I^* + k_1(\sigma+\eta I^*)},\\
V^* &= \frac{\phi\Lambda}{(\mu+\psi I^*)(\beta+k_1(\sigma+\eta I^*)},\\
I^* &= \frac{\alpha I^*}{k_3},\\
D^* &= \frac{\alpha I^*}{\mu+\pi\omega},\\
R^* &= \frac{(\gamma k_3+\alpha\omega)I^*}{\mu k_3},
\end{aligned}$$

4.3. **The Model's Basic Reproduction Number.** F and V are given as the matrix that is linearized of f and v at the DFE. The fundamental reproduction number [10], or is the parameter for the inhibit that controls the spread of a COVID-19 infection, and it was

obtained in this section. We employed the next-generation matrix approach [34, 35] to get the fundamental reproduction number, which is the spectral radius of the next-generation matrix. The rate of transmission (v) and the rate at which new infections could occur (f) from model system (3.1) are

$$F = \begin{bmatrix} \frac{\beta SI}{\sigma+\eta I} + \psi VI \\ 0 \end{bmatrix},$$

$$v = \begin{bmatrix} (\mu+\epsilon+\gamma)I + \alpha I \\ -\alpha I + (\mu+\pi+\omega)D \end{bmatrix},$$

$$F = \begin{bmatrix} \frac{\beta\Lambda}{\sigma(\phi+\mu)} + \frac{\phi\Lambda\psi}{\mu(\phi+\mu)} & 0 \\ 0 & 0 \end{bmatrix},$$

$$V = \begin{bmatrix} (\mu+\epsilon+\gamma+\alpha) & 0 \\ -\alpha & (\mu+\pi+\omega) \end{bmatrix},$$

The inverse of V is then found and provided by,

$$V^{-1} = \begin{bmatrix} \frac{1}{(\mu+\epsilon+\gamma+\alpha)} & 0 \\ \frac{\alpha}{(\mu+\pi+\omega)(\mu+\epsilon+\gamma+\alpha)} & \frac{1}{(\mu+\pi+\omega)} \end{bmatrix},$$

Finally,

$$FV^{-1} = \begin{bmatrix} \frac{\Lambda(\beta\mu+\phi\sigma\psi)}{\mu(\phi+\mu)(\alpha+\mu+\gamma+\epsilon)} & 0 \\ 0 & 0 \end{bmatrix},$$

The two eigenvalues of FV^{-1} are

$$\lambda_1 = 0,$$

$$\lambda_2 = \frac{\Lambda(\beta\mu+\phi\sigma\psi)}{\sigma\mu(\phi+\mu)(\alpha+\mu+\gamma+\epsilon)},$$

The spectral radius of FV^{-1} is

$$\rho FV^{-1} = R_0 = max[\lambda_1\lambda_2] = \frac{\Lambda(\beta\mu+\phi\sigma\psi)}{\sigma\mu(\phi+\mu)(\alpha+\mu+\gamma+\epsilon)}$$

4.4. **Sensitivity Analysis of R_0.**

$$R_0 = \frac{\Lambda(\beta\mu+\phi\sigma\psi)}{\sigma\mu(\phi+\mu)(\alpha+\mu+\gamma+\epsilon)}$$

$$\frac{\partial R_0}{\partial\Lambda} = \frac{\beta\mu+\phi\sigma\psi}{\sigma\mu(\phi+\mu)(\alpha+\mu+\gamma+\epsilon)} \times \frac{\Lambda}{R_0} < 1$$

$$\frac{\partial R_0}{\partial\beta} = \frac{\Lambda(\mu+\phi\sigma\psi)}{\sigma\mu(\phi+\mu)(\alpha+\mu+\gamma+\epsilon)} \times \frac{\beta}{R_0} < 1$$

$$\frac{\partial R_0}{\partial \psi} = \frac{\Lambda(\beta\mu + \phi\sigma)}{\sigma\mu(\phi+\mu)(\alpha+\mu+\gamma+\epsilon)} \times \frac{\psi}{R_0} < 1$$

$$\frac{\partial R_0}{\partial \alpha} = \frac{\Lambda(\beta\mu + \phi\psi\sigma)}{\sigma\mu(\phi+\mu)} \times \frac{\alpha}{R_0} < 1,$$

$$\frac{\partial R_0}{\partial \epsilon} = \frac{\Lambda(\beta\mu + \phi\sigma)}{\sigma\mu(\phi+\mu)} \times \frac{\epsilon}{R_0} > 1,$$

$$\frac{\partial R_0}{\partial \phi} = \frac{\sigma\mu((\phi+\mu)(\alpha+\gamma+\epsilon)\Lambda\sigma\psi - \Lambda\phi\sigma\psi(\sigma\mu(\sigma+\gamma+\epsilon))}{(\sigma\mu(\phi+\mu)(\alpha+\gamma+\epsilon))^2} \times \frac{\phi}{R_0} > 1,$$

$$\frac{\partial R_0}{\partial \mu} = \frac{\Lambda\beta\left(\sigma\mu\phi + \sigma\mu^2\right)(\alpha+\mu+\gamma+\epsilon) - \Lambda\beta\mu + \Lambda\phi\sigma\psi\,\Theta_\mu}{\left[(\sigma\mu\phi + \sigma\mu^2)(\alpha+\mu+\gamma+\epsilon)\right]^2} \cdot \frac{\mu}{R_0},$$

$$\frac{\partial R_0}{\partial \sigma} = \frac{\Lambda\phi\psi\left(\sigma\mu\phi + \sigma\mu^2\right)(\alpha+\mu+\gamma+\epsilon) - \Lambda\beta\mu + \Lambda\phi\sigma\psi\,\Theta_\sigma}{\left[(\sigma\mu\phi + \sigma\mu^2)(\alpha+\mu+\gamma+\epsilon)\right]^2} \cdot \frac{\sigma}{R_0},$$

TABLE 2. Sensitivity Index

Parameter	**Sensitivity Index**	**Effect on R_0**
Λ	1.00	Neutral/proportional
β	0.342	< 1
μ	1.925	> 1
σ	1.158	> 1
α	0.296	< 1
ψ	0.669	< 1
ϵ	2.442	> 1

5. Sensitivity Analysis and Parameter Significance

Significance analysis of the basic reproduction number R_0 highlights the relative impact of model parameters on disease transmission. The recruitment rate Λ, natural death rate μ, disease-induced removal rate ϵ, and progression rate from exposed to infectious σ are the most influential, with increase in these parameters substantially raising R_0. Moderate effects are observed for the transmission rate β and infectivity factor ψ, indicating that changes in contact or transmission probability can affect disease spread but to a lesser extent. Parameters such as the treatment/removal α have minor influence, while others, including ϕ, η, γ, π and ω exhibit negligible impact. These findings suggest that effective control strategies should prioritize interventions targeting ϵ, μ, σ and Λ to meaningfully reduce disease transmission.

6. Stability Analysis

Theorem 1. *The disease-free equilibrium point $E_f = (S, V, I, D, R)$ of system (3.1) is locally asymptotically stable whenever $R_0 < 1$ and unstable whenever $R_0 > 1$.*

Proof. At the disease-free equilibrium E_f the effect linearized matrix of system (3.1) is provided by

$$\begin{aligned}
\frac{dS}{dt} &= \Lambda - \frac{\beta SI}{\sigma + \eta I} - \Phi S - \mu S,\\
\frac{dV}{dt} &= \Phi S - (\mu + \psi I)V,\\
\frac{dI}{dt} &= \frac{\beta SI}{\sigma + \eta I} - \psi VI - (\mu + \epsilon + \gamma + \alpha)I,\\
\frac{dD}{dt} &= \alpha I - (\mu + \pi + \omega)D,\\
\frac{dR}{dt} &= \gamma I + \omega D - \mu R.
\end{aligned}$$

Taking partial derivative above equation (3.1),
i)

$$\frac{\partial S}{\partial t} = \Lambda - \frac{\beta SI}{\sigma + \eta I} - \Phi S - \mu S$$

$$\frac{\partial S}{\partial S} = -\frac{\beta I}{\sigma + \eta I} - \Phi - \mu, \qquad \frac{\partial S}{\partial I} = -\frac{\alpha\beta S}{(\sigma + \eta I)^2}$$

$$\frac{\partial S}{\partial D} = 0, \qquad \frac{\partial S}{\partial R} = 0, \qquad \frac{\partial S}{\partial V} = 0$$

ii)

$$\frac{\partial V}{\partial t} = \Phi S - (\mu + \psi I)V$$

$$\frac{\partial V}{\partial S} = \Phi, \qquad \frac{\partial V}{\partial V} = -(\mu + \psi I), \qquad \frac{\partial V}{\partial I} = -(V\psi)$$

$$\frac{\partial V}{\partial D} = 0, \qquad \frac{\partial V}{\partial R} = 0.$$

iii)

$$\frac{dI}{dt} = \frac{\beta SI}{\sigma + \eta I} - \psi VI - (\mu + \epsilon + \gamma + \alpha)I$$

$$\frac{\partial I}{\partial I} = \frac{\beta S}{(\sigma + \eta I)^2} - \psi V - (\mu + \epsilon + \gamma + \alpha)$$

$$\frac{\partial I}{\partial S} = \frac{\beta I}{\sigma + \eta I}, \qquad \frac{\partial I}{\partial V} = \psi I, \qquad \frac{\partial I}{\partial D} = \frac{\partial I}{\partial R} = 0$$

Now, solve next equation as well as solve above equation.
iv)

$$\frac{dD}{dt} = \alpha I - (\mu + \pi + \omega)D$$

$$\frac{\partial D}{\partial S} = \frac{\partial D}{\partial V} = \frac{\partial D}{\partial R} = 0$$

$$\frac{\partial D}{\partial I} = \alpha, \qquad \frac{\partial D}{\partial D} = -(14 + \pi + \omega)$$

v)

$$\frac{dR}{dt} = \gamma I + \omega D - \mu R, \qquad \frac{\partial R}{\partial S} = \frac{\partial R}{\partial V} = 0$$

$$\frac{\partial R}{\partial I} = \gamma, \qquad \frac{\partial R}{\partial D} = \omega, \qquad \frac{\partial R}{\partial R} = -\mu$$

Putting all values into the Jacobian matrix,

$$J(E_0) = \begin{bmatrix} -(\varphi+\mu) & 0 & \frac{\beta\Lambda}{\sigma(\varphi+\mu)} & 0 & 0 \\ \varphi & -\mu & -\frac{\psi\Lambda\varphi}{\mu(\varphi+\mu)} & 0 & 0 \\ 0 & 0 & \frac{\beta\Lambda}{\sigma(\varphi+\mu)} + \frac{\psi\Lambda\varphi}{\mu(\varphi+\mu)} - (\mu+\epsilon+\gamma) & 0 & 0 \\ 0 & 0 & \alpha & -(\mu+\pi+\omega) & 0 \\ 0 & 0 & \gamma & \omega & -\mu \end{bmatrix},$$

where

$$E_0 = \left(\frac{\Lambda}{\varphi+\mu}, \frac{\Lambda\varphi}{\mu(\varphi+\mu)}, 0, 0, 0\right).$$

Put all DFE values into the Jacobian matrix, where

$$k_1 = \varphi + \mu, \qquad k_2 = \mu + \epsilon + \sigma + \gamma, \qquad k_3 = \mu + \pi + \omega.$$

Then

$$J(E_0) = \begin{bmatrix} -k_1 & 0 & -\frac{\beta\Lambda}{\sigma k_1} & 0 & 0 \\ \varphi & -\mu & -\frac{\psi\varphi\Lambda}{\mu k_1} & 0 & 0 \\ 0 & 0 & \frac{\Lambda(\beta\mu+\varphi\sigma\psi)}{\sigma\mu k_1} - k_2 & 0 & 0 \\ 0 & 0 & \alpha & -k_3 & 0 \\ 0 & 0 & \gamma & \omega & -\mu \end{bmatrix}.$$

The characteristic equation is

$$|J(E_0) - \lambda I| = 0.$$

Hence,

$$\begin{vmatrix} -k_1-\lambda & 0 & -\dfrac{\beta\Lambda}{\sigma k_1} & 0 & 0 \\ \varphi & -\mu-\lambda & -\dfrac{\psi\varphi\Lambda}{\mu k_1} & 0 & 0 \\ 0 & 0 & \dfrac{\Lambda(\beta\mu+\varphi\sigma\psi)}{\sigma\mu k_1}-k_2-\lambda & 0 & 0 \\ 0 & 0 & \alpha & -k_3-\lambda & 0 \\ 0 & 0 & \gamma & \omega & -\mu-\lambda \end{vmatrix} = 0.$$

Therefore, the characteristic polynomial is

$$(\lambda+k_1)(\lambda+\mu)^2(\lambda+k_3)\left(\lambda-\frac{\Lambda(\beta\mu+\varphi\sigma\psi)}{\sigma\mu k_1}+k_2\right)=0.$$

Hence, the eigenvalues are

$$\lambda_1=-k_1, \qquad \lambda_2=-\mu, \qquad \lambda_3=-\mu, \qquad \lambda_4=-k_3,$$

and

$$\lambda_5=\frac{\Lambda(\beta\mu+\varphi\sigma\psi)}{\sigma\mu k_1}-k_2.$$

$$\begin{aligned}\lambda_5&=\frac{\Lambda(\beta\mu+\varphi\sigma\psi)}{\sigma\mu K_1}-(\mu+\gamma+\epsilon+\sigma)\\&=(\mu+\gamma+\epsilon+\sigma)\left(\frac{\Lambda(\beta\mu+\varphi\sigma\psi)}{\sigma\mu(\varphi+\mu)(\mu+\gamma+\epsilon+\sigma)}-1\right).\end{aligned}$$

We know that,

$$R_0=\frac{\Lambda(\beta\mu+\varphi\sigma\psi)}{\sigma\mu(\varphi+\mu)(\mu+\gamma+\epsilon+\sigma)}. \tag{6. 3}$$

Hence,

$$\lambda_5=(\mu+\gamma+\epsilon+\sigma)(R_0-1). \tag{6. 4}$$

□

6.1. **Local Stability at Endemic Equilibrium.**

$$A=\frac{\beta I^*}{\sigma+\eta I^*}, \qquad B=\frac{\sigma\beta S^*}{(\sigma+\eta I^*)^2},$$

$$J(E^*)=\begin{bmatrix} -(A+\varphi+\mu) & 0 & B & 0 & 0 \\ \varphi & -\mu+\psi I^* & -\psi V^* & 0 & 0 \\ A & \psi I^* & B+\psi V^*-(\mu+\epsilon+\gamma) & 0 & 0 \\ 0 & 0 & \alpha & -(\mu+\pi+\omega) & 0 \\ 0 & 0 & \gamma & \omega & -\mu \end{bmatrix}.$$

where

$$K_1 = -\frac{\beta I^*}{\sigma + \eta I^*} - \varphi - \mu,$$

$$K_2 = \frac{\sigma\beta S^*}{(\sigma + \eta I^*)^2}, \qquad K_3 = -\mu + \psi I^*, \qquad K_4 = \frac{\beta I^*}{\sigma + \eta I^*},$$

$$K_5 = \frac{\sigma\beta S^*}{(\sigma + \eta I^*)^2} + \psi V^* - (\mu + \epsilon + \gamma), \qquad K_6 = -(\mu + \pi + \omega).$$

Hence,

$$J(E^*) = \begin{bmatrix} K_1 & 0 & K_2 & 0 & 0 \\ \varphi & K_3 & -V^*\psi & 0 & 0 \\ K_4 & \psi I^* & K_5 & 0 & 0 \\ 0 & 0 & \alpha & K_6 & 0 \\ 0 & 0 & \gamma & \gamma & -\mu \end{bmatrix}.$$

The characteristic equation is

$$|J(E^*) - \lambda I| = 0.$$

That is,

$$\begin{vmatrix} K_1 - \lambda & 0 & K_2 & 0 & 0 \\ \varphi & K_3 - \lambda & -V^*\psi & 0 & 0 \\ K_4 & \psi I^* & K_5 - \lambda & 0 & 0 \\ 0 & 0 & \alpha & K_6 - \lambda & 0 \\ 0 & 0 & \gamma & \gamma & -\mu - \lambda \end{vmatrix} = 0.$$

Expanding the determinant gives

$$-\mu - \lambda = 0,$$

which implies

$$\lambda = -\mu.$$

Also,

$$K_6 - \lambda = 0,$$

so that

$$\lambda = K_6.$$

The remaining characteristic determinant is

$$\begin{vmatrix} K_1 - \lambda & 0 & K_2 \\ \varphi & K_3 - \lambda & -V^*\psi \\ K_4 & \psi I^* & K_5 - \lambda \end{vmatrix} = 0.$$

By solving, we obtain

$$-\lambda^3 + \lambda^2(K_1 + K_3 + K_5) - \lambda\left(K_1K_3 + K_1K_5 + K_3K_5 + V^*I^*\psi^2 - K_2K_4\right)$$

$$+K_1K_3K_5 + K_4V^*I^*\psi^2 + K_2\varphi\psi I^* - K_2K_3K_4 = 0.$$

Equivalently,

$$-\lambda^3 + a_2\lambda^2 - a_1\lambda + a_0 = 0,$$

or

$$\lambda^3 - a_2\lambda^2 - a_1(-\lambda) - a_0 = 0.$$

According to the Routh–Hurwitz criterion [31], all roots of the characteristic equation have negative real parts. Therefore, the endemic equilibrium point E^* is locally asymptotically stable.

6.2. **Global Stability.**

Theorem 2. *The disease-free equilibrium (DFE) point*

$$E_f = \left(\frac{\Lambda}{\phi + \mu}, \frac{\Lambda\phi}{\mu(\mu + \phi)}, 0, 0, 0\right)$$

of the given system is globally asymptotically stable when $R_0 < 1$ *and unstable when* $R_0 > 1$.

Proof. Consider a Volterra-type Lyapunov function [32]

$$U : \Omega \to \mathbb{R},$$

defined by

$$U = (S - S^0 \ln S) + V + I + D + R.$$

Computing the time derivative of U,

$$\dot{U} = \left(1 - \frac{S^0}{S}\right)\dot{S} + \left(1 - \frac{V^0}{V}\right)\dot{V} + \dot{I} + \dot{D} + \dot{R}.$$

Substituting the model equations gives

$$\dot{S} = \Lambda - \frac{\beta SI}{\sigma + \eta I} - \phi S - \mu S,$$

$$\dot{V} = \phi S - V(\mu + \psi I),$$

$$\dot{I} = \frac{\beta SI}{\sigma + \eta I} + \psi VI - (\mu + \epsilon + \gamma)I - \alpha I,$$

$$\dot{D} = \alpha I - (\mu + \pi + \omega)D,$$

$$\dot{R} = \gamma I + \omega D - \mu R.$$

Substituting these expressions into $\dot{U}$, we obtain

$$\begin{aligned}\dot{U} = & \left(1 - \frac{S^0}{S}\right)\left(\Lambda - \frac{\beta SI}{\sigma + \eta I} - \phi S - \mu S\right) \\ & + \left(1 - \frac{V^0}{V}\right)(\phi S - V(\mu + \psi I)) \\ & + \left(\frac{\beta SI}{\sigma + \eta I} + \psi VI - (\mu + \epsilon + \gamma)I - \alpha I\right) \\ & + (\alpha I - (\mu + \pi + \omega)D) + (\gamma I + \omega D - \mu R)\,.\end{aligned}$$

Let,

$$S^0 = \frac{\Lambda}{\phi + \mu} \quad \text{and} \quad V^0 = \frac{\Lambda\phi}{(\mu + \phi)}.$$

Then, $\dot{U}$ is simplified into

$$\dot{U} = \frac{\mu}{S}(S - S^0) + \frac{\mu}{V}(V - V^0) - (\mu + \epsilon + \gamma)I - (\mu + \pi + \omega)D - \mu R.$$

We now analyze $\dot{U}$. For $R_0 < 1$, we have

$$\frac{\beta}{\sigma + \eta I} < \mu, \qquad \text{and} \qquad \phi < \mu.$$

Thus,

$$\dot{U} \leq 0.$$

Equality holds ($\dot{U} = 0$) if and only if

$$S = S^0, \qquad V = V^0, \qquad I = 0, \qquad D = 0, \qquad R = 0.$$

Hence, the DFE E_f is GAS when $R_0 < 1$. □

Theorem 3. *For $R_0 > 1$, the system is GAS at the EE point.*

Proof. Suppose $R_0 > 1$. The Lyapunov function $\mathcal{L} : \mathbb{R}^5_+ \to \mathbb{R}_+$ is constructed by the following formula:

$$\mathcal{L} = \frac{1}{2}\left[(S - S^*)^2 + (V - V^*)^2 + (I - I^*)^2 + (D - D^*)^2 + (R - R^*)^2\right].$$

Then,

$$\dot{\mathcal{L}} = (S - S^*)\dot{S} + (V - V^*)\dot{V} + (I - I^*)\dot{I} + (D - D^*)\dot{D} + (R - R^*)\dot{R}.$$

Substitute the ODEs and use equilibrium conditions.

$$\dot{\mathcal{L}} = -\mu(S-S^*)^2 - \mu(V-V^*)^2 - (\mu+\epsilon)(I-I^*)^2 - (\mu+\pi)(D-D^*)^2 - \mu(R-R^*)^2 + \text{terms involving } \frac{\beta SI}{\sigma+\eta I} \text{ and } \psi IV.$$

Using the fact that at equilibrium,

$$\frac{\beta S^*}{\sigma+\eta I^*} + \psi V^* = \mu + \epsilon + \gamma + \alpha,$$

one can show that the infection terms combine into negative semidefinite expressions when $R_0 > 1$ (because the endemic equilibrium exists and is unique). :::writingvariant="document" id="63481"

$$\dot{\mathcal{L}} = -\mu(S-S^*)^2 - \mu(V-V^*)^2 - (\mu+\epsilon)(I-I^*)^2 - (\mu+\pi)(D-D^*)^2 - \mu(R-R^*)^2 - \frac{\beta\alpha S^* I^*}{\sigma+\eta I^*}(I-I^*)^2,$$

Thus,

$$\dot{\mathcal{L}} \leq 0,$$

and

$$\dot{\mathcal{L}} = 0 \quad \text{if and only if} \quad S = S^*,\ V = V^*,\ I = I^*,\ D = D^*,\ R = R^*.$$

Hence, for $R_0 > 1$, the endemic equilibrium (EE) is globally asymptotically stable (GAS) in the interior of the feasible region. □

7. Numerically Analysis of Mathematical System

In the present section, many discrete techniques with respect the continuous structure (1) are developed. The main objective to obtain an extensive understanding of the dynamics of COVID-19 immunization and treatment. The Euler, RK 4, and NSFD strategy are the three schemes that are constructed [36, 37]. It has been shown that the NSFD scheme is not only free from dependence on the step size but also outperforms the other schemes in all aspects.

7.1. **Euler Scheme.**

The Euler scheme for Above System can be constructed using the following procedures.
(i)

$$\frac{\partial S}{\partial t} = \Lambda - \frac{\beta SI}{\sigma+\eta I} - \Phi S - \mu S$$

$$\frac{S^{K+1}-S^K}{h} = \Lambda - \frac{\beta S^K I^K}{\sigma+\eta I^K} - \Phi S^K - \mu S^K$$

$$S^{K+1} = S^K + h\left[\Lambda - \frac{\beta S^K I^K}{\sigma+\eta I^K} - \Phi S^K - \mu S^K\right].$$

(ii)

$$\frac{\partial V}{\partial t} = \Phi S - (\mu + \psi I)V,$$

$$\frac{V^{K+1} - V^K}{h} = \Phi S^K - (\mu + \psi I^K)V^K,$$

$$V^{K+1} = V^K + h[\Phi S^K - (\mu + \psi I^K)V^K],$$

(iii)

$$\frac{\partial I}{\partial t} = \frac{\beta SI}{\sigma + \eta I} - \psi VI - (\mu + \epsilon + \gamma + \alpha)I$$

$$\frac{I^{K+1} - I^K}{h} = \frac{\beta S^K I^K}{\sigma + \eta I^K} - \psi V^K I^K - (\mu + \epsilon + \gamma + \alpha)I^K$$

$$I^{K+1} = I^K + h[\frac{\beta S^K I^K}{\sigma + \eta I^K} - \psi V^K I^K - (\mu + \epsilon + \gamma + \alpha)I^K]$$

(iv)

$$\frac{\partial D}{\partial t} = \alpha I - (\mu + \pi + \omega)D$$

$$\frac{D^{K+1} - D^K}{h} = \alpha I^K - (\mu + \pi + \omega)D^K$$

$$D^{K+1} = D^K + h[\alpha I^K - (\mu + \pi + \omega)D^K]$$

(v)

$$\frac{\partial R}{\partial t} = \gamma I + \omega D - \mu R$$

$$\frac{R^{K+1} - R^K}{h} = \gamma I^K + \omega D^K - \mu R^K$$

$$R^{K+1} = R^K + h[\gamma I^K + \omega D^K - \mu R^K]$$

Therefore, the Euler scheme becomes,

$$S^{K+1} = S^K + h\left[\Lambda - \frac{\beta S^K I^K}{\sigma + \eta I^K} - \Phi S^K - \mu S^K\right],$$

$$V^{K+1} = V^K + h[\Phi S^K - (\mu + \psi I^K)V^K],$$

$$I^{K+1} = I^K + h[\frac{\beta S^K I^K}{\sigma + \eta I^K} - \psi V^K I^K - (\mu + \epsilon + \gamma + \alpha)I^K],$$

$$D^{K+1} = D^K + h[\alpha I^K - (\mu + \pi + \omega)D^K],$$

$$R^{K+1} = R^K + h[\gamma I^K + \omega D^K - \mu R^K].$$

As Figure 2 (a-c) illustrates, the Euler scheme's numerical solutions are positive once the step size is short. As demonstrated in Figure 2(d), stability lost as the step-size increases. Therefore, Euler scheme's positivity and stability are broken all finite step sizes.

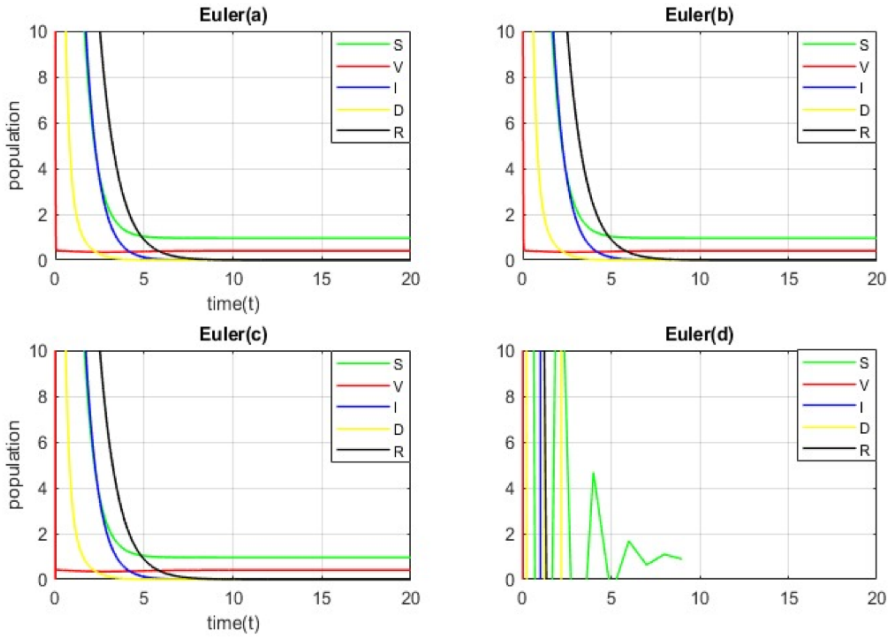

FIGURE 2. Graphs generated by the Euler method

Figure 2. Graphs generated by the Euler method (7.1) with (a) $h = 0.0001$, (b) $h = 0.001$ (c) $h = 0.01$ and (d) $h = 0.1$. The remaining value of the parameters are offered as $\Lambda = 1.3703, \beta = 0.0108, \psi = 0.01, \phi = 0.43, \gamma = 0.1, \alpha = 0.22, \sigma = 0.22, \epsilon = 0.0271, \eta = 1, \pi = 1, \mu = 1, \omega = 0.2$

7.2. **Fourth-order Runge-Kutta Scheme.** To develop the RK-4 scheme, it is assumed that $S = l, V = m, I = n, D = p$ and $R = q$. Then, the RK-4 scheme is described four stages as follows:

Stage 1.

$$l_1 = h[\Lambda - \frac{\beta S^k I^k}{\sigma + \eta I^k} - \phi S^k - \mu S^k]$$

$$m_1 = h[\phi S^k - (\mu + \psi I^k)V^k]$$

$$n_1 = h\left[\frac{\beta S^k I^k}{\sigma + \eta I^k} + \psi V^k I^k - (\mu + \epsilon + \gamma)I^k - \alpha I^k\right]$$

$$p_1 = h\left[\alpha I^k - (\mu+\pi+\omega)D^k\right]$$

$$q_1 = h\left[\gamma I^k + \omega D^k - \mu R^k\right]$$

Stage 2.

$$l_2 = h\left[\Lambda - \frac{\beta\left(S^k+\frac{l_1}{2}\right)\left(I^k+\frac{n_1}{2}\right)}{\sigma+\eta\left(I^k+\frac{n_1}{2}\right)} - \varphi\left(S^k+\frac{l_1}{2}\right) - \mu\left(S^k+\frac{l_1}{2}\right)\right],$$

$$m_2 = h\left[\varphi\left(S^k+\frac{l_1}{2}\right) - \left(\mu+\psi\left(I^k+\frac{n_1}{2}\right)\right)\left(V^k+\frac{m_1}{2}\right)\right]$$

$$n_2 = h\left[\frac{\beta\left(S^k+\frac{l_1}{2}\right)\left(I^k+\frac{n_1}{2}\right)}{\sigma+\eta\left(I^k+\frac{n_1}{2}\right)} + \psi\left(V^k+\frac{m_1}{2}\right)\left(I^k+\frac{n_1}{2}\right) - (\mu+\epsilon+\gamma)\left(I^k+\frac{n_1}{2}\right) - \alpha\left(I^k+\frac{n_1}{2}\right)\right],$$

$$p_2 = h\left[\alpha\left(I^k+\frac{n_1}{2}\right) - (\mu+\pi+\omega)\left(D^k+\frac{p_1}{2}\right)\right],$$

$$q_2 = h\left[\gamma\left(I^k+\frac{n_1}{2}\right) + \omega\left(D^k+\frac{p_1}{2}\right) - \mu\left(R^k+\frac{q_1}{2}\right)\right].$$

Stage 3.

$$l_3 = h\left[\Lambda - \frac{\beta\left(S^k+\frac{l_2}{2}\right)\left(I^k+\frac{n_2}{2}\right)}{\sigma+\eta\left(I^k+\frac{n_2}{2}\right)} - \varphi\left(S^k+\frac{l_2}{2}\right) - \mu\left(S^k+\frac{l_2}{2}\right)\right],$$

$$m_3 = h\left[\varphi\left(S^k+\frac{l_2}{2}\right) - \left(\mu+\psi\left(I^k+\frac{n_2}{2}\right)\right)\left(V^k+\frac{m_2}{2}\right)\right]$$

$$n_3 = h\left[\frac{\beta\left(S^k+\frac{l_2}{2}\right)\left(I^k+\frac{n_2}{2}\right)}{\sigma+\eta\left(I^k+\frac{n_2}{2}\right)} + \psi\left(V^k+\frac{m_2}{2}\right)\left(I^k+\frac{n_2}{2}\right) - (\mu+\epsilon+\gamma)\left(I^k+\frac{n_2}{2}\right) - \alpha\left(I^k+\frac{n_2}{2}\right)\right],$$

$$p_3 = h\left[\alpha\left(I^k+\frac{n_2}{2}\right) - (\mu+\pi+\omega)\left(D^k+\frac{p_2}{2}\right)\right],$$

$$q_3 = h\left[\gamma\left(I^k+\frac{n_2}{2}\right) + \omega\left(D^k+\frac{p_2}{2}\right) - \mu\left(R^k+\frac{q_2}{2}\right)\right].$$

Stage 4.

$$l_4 = h\left[\Lambda - \frac{\beta\left(S^k + l_3\right)\left(I^k + n_3\right)}{\sigma + \eta\left(I^k + n_3\right)} - \varphi\left(S^k + l_3\right) - \mu\left(S^k + l_3\right)\right],$$

$$m_4 = h\left[\varphi\left(S^k + l_3\right) - \left(\mu + \psi\left(I^k + n_3\right)\right)\left(V^k + m_3\right)\right],$$

$$n_4 = h\left[\frac{\beta\left(S^k + l_3\right)\left(I^k + n_3\right)}{\sigma + \eta\left(I^k + n_3\right)} + \psi\left(V^k + m_3\right)\left(I^k + n_3\right) - (\mu + \epsilon + \gamma)\left(I^k + n_3\right) - \alpha\left(I^k + n_3\right)\right],$$

$$p_4 = h\left[\alpha\left(I^k + n_3\right) - (\mu + \pi + \omega)\left(D^k + p_3\right)\right],$$

$$q_4 = h\left[\gamma\left(I^k + n_3\right) + \omega\left(D^k + p_3\right) - \mu\left(R^k + q_3\right)\right].$$

Finally, the numerical approximations are

$$S^{k+1} = S^k + \frac{1}{6}\left(l_1 + 2l_2 + 2l_3 + l_4\right),$$

$$V^{k+1} = V^k + \frac{1}{6}\left(m_1 + 2m_2 + 2m_3 + m_4\right)$$

$$I^{k+1} = I^k + \frac{1}{6}\left(n_1 + 2n_2 + 2n_3 + n_4\right),$$

$$D^{k+1} = D^k + \frac{1}{6}\left(p_1 + 2p_2 + 2p_3 + p_4\right),$$

$$R^{k+1} = R^k + \frac{1}{6}\left(q_1 + 2q_2 + 2q_3 + q_4\right).$$

Figure 3. Graphs initiate by the RK-4 method (7.2) (a) $h = 0.0001, (b)h = 0.001(c)h = 0.01and(d)h = 0.1$. The left value of the parameters offered as $\Lambda = 1.3703, \beta = 0.0108, \psi = 0.01, \phi = 0.43, \gamma = 0.1, \alpha = 0.22, \sigma = 0.22, \epsilon = 0.0271, \eta = 1, \pi = 1, \mu = 1, \omega = 0.2$. Figure 3 (a-d) is a graphic representation of the RK-4 scheme (7.2). The graphs produced by using the RK-4 strategy are positive and convergent for small step sizes, as seen in Figure 3 (a-c). As the step size increases, the RK 4 scheme diverges for large values of h, as Figure 3 (d) illustrates, breaking the stability of model (3.1).

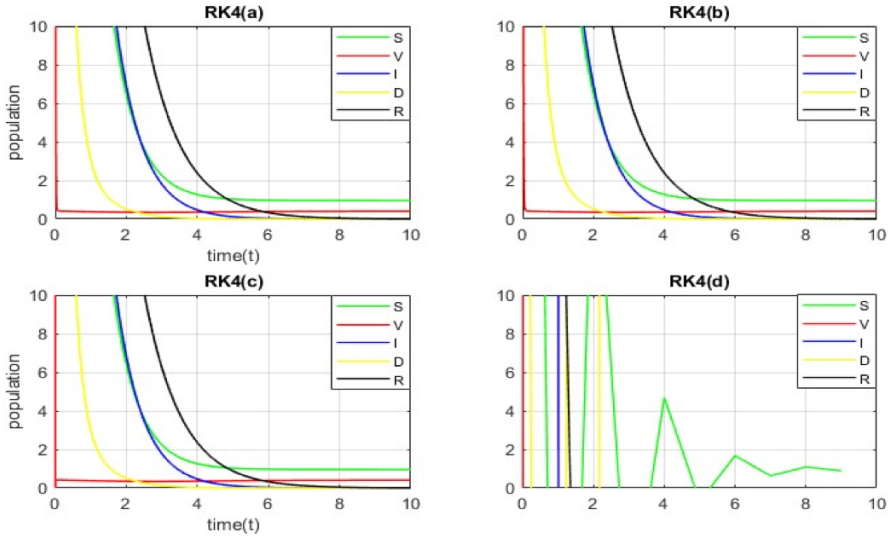

FIGURE 3. Graphs initiate by the RK-4 method

7.3. **Non-Standard Finite Difference (NSFD) Scheme.** Mickens [38] generate the NSFD scheme which approximates solutions of the ordinary and partial differential equations. According to Shokri et al. [39], there are two factors affect the study of the NSFD scheme. The first how to discretize the derivative and the second constitutes the best way to approximate the nonlinear terms. The forward finite difference approximation is one of the general methods of first order derivative discretization. The first order derivative $\frac{dy}{dx}$ is written in standard form as $\frac{y(x+h)-y(x)}{h}$, where h stands for the step size. According to Mickens, this can be expressed as, where h is referred to as the denominator function. There are various formulas for $\phi(h)$ that can be viewed in [39]. In the current paper $\phi(h) = h$. To build the NSFD scheme for the system, conduct the subsequent actions.

$$\frac{S^{k+1} - S^k}{h} = \Lambda - \frac{\beta S^{k+1} I^k}{\sigma + \eta I^k} - \varphi S^{k+1} - \mu S^{k+1},$$

$$\frac{V^{k+1} - V^k}{h} = \varphi S^k - (\mu + \psi I^k) V^{k+1},$$

$$\frac{I^{k+1} - I^k}{h} = \frac{\beta S^k I^{k+1}}{\sigma + \eta I^{k+1}} + \psi V I^{k+1} - (\mu + \epsilon + \gamma) I^{k+1} - \alpha I^{k+1},$$

$$\frac{D^{k+1} - D^k}{h} = \alpha I^k - (\mu + \pi + \omega) D^{k+1},$$

$$\frac{R^{k+1}-R^k}{h}=\gamma I^k+\omega D^k-\mu R^{k+1}.$$

The above equations can rewrite as

$$S^{k+1}=\frac{h\Lambda+S^k}{1+h\mu+h\varphi+\dfrac{h\beta I^k}{\sigma+\eta I^k}},$$

$$V^{k+1}=\frac{h\varphi S^k+V^k}{1+h(\mu+\psi I^k)},$$

$$I^{k+1}=\frac{I^k+\dfrac{h\beta S^k I^{k+1}}{\sigma+\eta I^{k+1}}}{1-h\left(\psi V^k-(\mu+\epsilon+\gamma)-\alpha\right)},$$

$$D^{k+1}=\frac{D^k+h\alpha I^k}{1+h(\mu+\pi+\omega)},$$

$$R^{k+1}=\frac{h\gamma I^k+h\omega D^k+R^k}{1+h\mu}.$$

7.4. **Stability Analysis of DFE and Endemic Point Using Discrete NSFD Scheme.** Examining the stability of equilibrium points for the NSFD method. To analyze local stability, assume.

$$A=S^{k+1}=\frac{h\Lambda+S^k}{1+h\mu+h\varphi+\dfrac{h\beta I^k}{\sigma+\eta I^k}},$$

$$B=V^{k+1}=\frac{h\varphi S^k+V^k}{1+h(\mu+\psi I^k)},$$

$$C=I^{k+1}=\frac{I^k+\dfrac{h\beta S^k I^{k+1}}{\sigma+\eta I^{k+1}}}{1-h\left(\psi V^k-(\mu+\epsilon+\gamma)-\alpha\right)},$$

$$F=D^{k+1}=\frac{D^k+h\alpha I^k}{1+h(\mu+\pi+\omega)},$$

$$E=R^{k+1}=\frac{h\gamma I^k+h\omega D^k+R^k}{1+h\mu}.$$

We will use the Schur Cohn condition [40] to show DFE and DEF points LAS as mentioned in lemma.

7.5. **Lemma.** The roots of the equation

$$\lambda^2 - T\lambda + D = 0$$

ensure $|\lambda_i| < 1,\ i = 1, 2$ if and only if the following requirements are fulfilled.

(i) $1 + T + D > 0$,
(ii) $1 - T + D > 0$,
(iii) $D < 1$.

The Jacobian matrix Trace and determinant are denoted by T and D, respectively.

Theorem 4. *The DFE point E_0 for the discrete NSFD scheme is LAS if $R_0 < 1$.*

Proof. Let's examine the Jacobian matrix,

$$J = \begin{bmatrix} \frac{\partial A}{\partial S} & \frac{\partial A}{\partial V} & \frac{\partial A}{\partial I} & \frac{\partial A}{\partial D} & \frac{\partial A}{\partial R} \\ \frac{\partial B}{\partial S} & \frac{\partial B}{\partial V} & \frac{\partial B}{\partial I} & \frac{\partial B}{\partial D} & \frac{\partial B}{\partial R} \\ \frac{\partial C}{\partial S} & \frac{\partial C}{\partial V} & \frac{\partial C}{\partial I} & \frac{\partial C}{\partial D} & \frac{\partial C}{\partial R} \\ \frac{\partial F}{\partial S} & \frac{\partial F}{\partial V} & \frac{\partial F}{\partial I} & \frac{\partial F}{\partial D} & \frac{\partial F}{\partial R} \\ \frac{\partial E}{\partial S} & \frac{\partial E}{\partial V} & \frac{\partial E}{\partial I} & \frac{\partial E}{\partial D} & \frac{\partial E}{\partial R} \end{bmatrix}.$$

We first find out all the derivatives of the above Jacobian matrix, as follows.

$$A = \frac{h\Lambda + S^k}{1 + \dfrac{h\beta I^k}{\sigma + \eta I^k} + h(\varphi + \mu)}.$$

$$\frac{\partial A}{\partial S} = \frac{1}{1 + \dfrac{h\beta I}{\sigma + \eta I} + h(\varphi + \mu)},$$

$$\frac{\partial A}{\partial I} = -\frac{(h\Lambda + S)\left(\dfrac{h\beta(\sigma + \eta) - h\beta\eta I}{(\sigma + \eta I)^2}\right)}{\left(1 + \dfrac{h\beta I}{\sigma + \eta I} + h(\varphi + \mu)\right)^2},$$

$$\frac{\partial A}{\partial D} = 0, \qquad \frac{\partial A}{\partial R} = 0, \qquad \frac{\partial A}{\partial V} = 0,$$

$$B = \frac{h\varphi S^k + V^k}{1 + h(\mu + \psi I^k)}, \qquad \frac{\partial B}{\partial S} = \frac{h\varphi}{1 + h(\mu + \psi I)},$$

$$\frac{\partial B}{\partial V} = \frac{1}{1 + h(\mu + \psi I)}, \qquad \frac{\partial B}{\partial I} = -\frac{(h\varphi S + V)(h\psi)}{(1 + h(\mu + \psi I))^2},$$

$$\frac{\partial B}{\partial D} = 0, \qquad \frac{\partial B}{\partial R} = 0.$$

Similarly find the other three derivatives as

$$C = \frac{I^k + \dfrac{h\beta S^k I^{k+1}}{\sigma + \eta I^{k+1}}}{1 - h\left(\psi V^k - (\mu + \epsilon + \gamma) - \alpha\right)}$$

$$\frac{\partial C}{\partial S} = \frac{\dfrac{h\beta I}{\sigma + \eta I}}{1 - h(\psi V - (\mu + \epsilon + \gamma) - \alpha)},$$

$$\frac{\partial C}{\partial V} = -\frac{(I + h\beta S)(h\psi)}{(1 - h(\psi V - (\mu + \epsilon + \gamma) - \alpha))^2},$$

$$\frac{\partial C}{\partial I} = \frac{1 + \dfrac{\sigma h\beta S}{(\sigma + \eta I)^2}}{1 - h(\psi V - (\mu + \epsilon + \gamma) - \alpha)},$$

$$\frac{\partial C}{\partial D} = 0, \qquad \frac{\partial C}{\partial R} = 0.$$

$$F = \frac{D^K + haI^K}{1 + h(\mu + \pi + \omega)}$$

$$\frac{\partial F}{\partial S} = 0, \quad \frac{\partial F}{\partial V} = 0, \quad \frac{\partial F}{\partial I} = \frac{ha}{1 + h(\mu + \pi + \omega)}, \quad \frac{\partial F}{\partial D} = \frac{1}{1 + h(\mu + \pi + \omega)},$$

$$E = \frac{hyI^K + h\omega D^K + R^K}{1 + h\mu}, \qquad \frac{\partial F}{\partial R} = 0.$$

$$\frac{\partial E}{\partial S} = 0, \quad \frac{\partial E}{\partial V} = 0, \quad \frac{\partial E}{\partial I} = \frac{hy}{1 + h\mu}, \quad \frac{\partial E}{\partial D} = \frac{h\omega}{1 + h\mu}, \quad \frac{\partial E}{\partial R} = \frac{1}{1 + h\mu}.$$

Now, we are putting all derivatives value such as

$$J(E) = \begin{bmatrix} \frac{1}{1 + \frac{h\beta I}{\sigma + \eta I} + h(\phi + \mu)} & 0 & \frac{(h\Lambda + hS)(2h\eta I\beta + \sigma)}{\left(1 + \frac{h\beta I}{\sigma + \eta I} + h(\phi + \mu)\right)^2 (\sigma + \eta I)^2} & 0 & 0 \\ \frac{h\phi}{1 + h(\mu + \psi)} & \frac{1}{1 + h(\mu + \psi)} & \frac{(h\phi S + V)(h\psi)}{(1 + h(\mu + \psi))^2} & 0 & 0 \\ \frac{\frac{h\beta I}{\sigma + \eta I}}{1 - h(\psi V - (\mu + \epsilon + \gamma) - \alpha)} & \frac{-\sigma + h\beta S}{(\sigma + \eta I)(1 - h(\psi V - (\mu + \epsilon + \gamma) - \alpha))^2} & \frac{\sigma h\beta S}{1 - h(\psi V - (\mu + \epsilon + \gamma) - \alpha)} & 0 & 0 \\ 0 & 0 & \frac{h\alpha}{1 + h(\mu + \pi + \omega)} & \frac{1}{1 + h(\mu + \pi + \omega)} & 0 \\ 0 & 0 & \frac{h\gamma}{1 + h\mu} & \frac{h\omega}{1 + h\mu} & \frac{1}{1 + h\mu} \end{bmatrix}$$

Point from Disease Free Equilibrium

$$S = \frac{\Lambda}{\phi+\mu}, \qquad V = \frac{\Lambda\phi}{\mu(\mu+\phi)}, \qquad I = 0, \qquad D = 0, \qquad R = 0.$$

Put all DFE in matrix (J), where

$$K_1 = \frac{1}{1+h(\phi+\mu)}, \qquad K_2 = \frac{h\Lambda + \dfrac{A\phi}{\phi+\mu}\,a}{1+h(\phi+\mu)^2},$$

$$K_3 = \frac{h\phi}{1+h\mu}, \qquad K_4 = \frac{1}{1+h\mu},$$

$$K_5 = h\left(\frac{\Lambda}{\phi+\mu} + \frac{\Lambda\phi}{\mu(\mu+\phi)}\right)\psi,$$

$$K_6 = \frac{1+\dfrac{h\beta\Lambda}{\sigma(\phi+\mu)}}{1+h\left(\phi\mu\left(\dfrac{\Lambda\phi}{\mu+\phi}\right)-(\mu+\epsilon+\gamma)-\alpha\right)},$$

$$K_7 = \frac{ha}{1+h(\mu+\pi+\omega)}, \qquad K_8 = \frac{1}{1+h(\mu+\pi+\omega)},$$

$$K_9 = \frac{hy}{1+h\mu}, \qquad K_{10} = \frac{h\omega}{1+h\mu}, \qquad K_{11} = \frac{1}{1+h\mu}.$$

$$J(E_0) = \begin{bmatrix} K_1 & 0 & K_2 & 0 & 0 \\ K_3 & K_4 & K_5 & 0 & 0 \\ 0 & 0 & K_6 & 0 & 0 \\ 0 & 0 & K_7 & K_8 & 0 \\ 0 & 0 & K_9 & K_{10} & K_{11} \end{bmatrix}$$

$$|J(E_0) - \lambda I| = 0$$

$$\begin{vmatrix} K_1-\lambda & 0 & K_2 & 0 & 0 \\ K_3 & K_4-\lambda & K_5 & 0 & 0 \\ 0 & 0 & K_6-\lambda & 0 & 0 \\ 0 & 0 & K_7 & K_8-\lambda & 0 \\ 0 & 0 & K_9 & K_{10} & K_{11}-\lambda \end{vmatrix} = 0$$

Hence,

$$K_{11} - \lambda = 0,$$

$$\lambda = K_{11},$$

$$K_8 - \lambda = 0,$$

$$\lambda = K_8,$$

$$K_6 = \lambda.$$

We consider the other two eigenvalues and discuss them.

$$\begin{vmatrix} K_1 - \lambda & 0 \\ K_3 & K_4 - \lambda \end{vmatrix} = 0 \tag{2}$$

From equation (2), we obtain

$$\lambda^2 - \lambda(K_1 + K_4) + K_1 K_4 = 0. \tag{3}$$

Comparing equation (3) with

$$\lambda^2 - T\lambda + D = 0,$$

we obtain

$$T = K_1 + K_4, \qquad D = K_1 K_4.$$

If $R_0 < 1$, then

$$T > 0, \qquad D > 0.$$

Then any of three conditions of Lemma are satisfied, i.e.
$1 + T + D > 0$ and $1 + K_1 + K_4 + K_1 K_4 > 0$

(i) $1 - T + D > 0$, then $1 - K_1 + K_4 + K_1 K_4 < 0$
(ii) $D < 1$. then $K_1 K_4 < 1$

All of the Schur-Cohn requirements stated in lemma are therefore satisfied whenever $R_0 < 1$. Consequently, the DFE point E_0 of discrete NSD schme is LAS, assuming that $R_0 < 1$. When a disease is worldwide in the population. It will continue to exist in such a community. The following theorem will examine if DEE point E^* is LAS using the Routh-Hurwitz criterion [40]. □

Theorem 5. *The DEE point E^* of the NSFD model is local stability analysis whenever $R_0 > 1$.*

Proof. The Jacobian matrix is obtained as per Theorem 4.

$$J(E) = \begin{bmatrix} \frac{1}{1 + \frac{h\beta I}{\sigma + \eta I} + h(\phi + \mu)} & 0 & \frac{(h\Lambda + S)(2h\eta\beta I + \sigma)}{\left(1 + \frac{h\beta I}{\sigma + \eta I} + h(\phi + \mu)\right)^2 (\sigma + \eta I)^2} & 0 & 0 \\ \frac{h\phi}{1 + h(\mu + \psi I)} & \frac{1}{1 + h(\mu + \psi I)} & \frac{(h\phi S + V)\, h\psi}{(1 + h(\mu + \psi I))^2} & 0 & 0 \\ \frac{\frac{h\beta I}{\sigma + \eta I}}{1 - h\left(\psi V - (\mu + \epsilon + \gamma) - \alpha\right)} & \frac{-\frac{1 + h\beta S}{(\sigma + \eta I)\, h\psi}}{\left(1 - h\left(\psi V - (\mu + \epsilon + \gamma) - \alpha\right)\right)^2} & \frac{\sigma h\beta S}{1 - h\left(\psi V - (\mu + \epsilon + \gamma) - \alpha\right)} & 0 & 0 \\ 0 & 0 & \frac{h\alpha}{1 + h(\mu + \pi + \omega)} & \frac{1}{1 + h(\mu + \pi + \omega)} & 0 \\ 0 & 0 & \frac{h\gamma}{1 + h\mu} & \frac{h\omega}{1 + h\mu} & \frac{1}{1 + h\mu} \end{bmatrix} \tag{7. 5}$$

By Putting the DEE point E^*, we obtain,

$$J(E^*) = \begin{bmatrix} \frac{1}{1+\frac{h\beta I^*}{\sigma+\eta I^*}+h(\phi+\mu)} & 0 & \frac{(h\Lambda+S^*)(2h\eta\beta I^*+\sigma)}{\left(1+\frac{h\beta I^*}{\sigma+\eta I^*}+h(\phi+\mu)\right)^2(\sigma+\eta I^*)^2} & 0 & 0 \\ \frac{h\phi}{1+h(\mu+\psi I^*)} & \frac{1}{1+h(\mu+\psi I^*)} & \frac{(h\phi S^*+V^*)h\psi}{(1+h(\mu+\psi I^*))^2} & 0 & 0 \\ \frac{\frac{h\beta I^*}{\sigma+\eta I^*}}{1-h(\psi V^*-(\mu+\epsilon+\gamma)-\alpha)} & \frac{-\frac{1+h\beta S^*}{(\sigma+\eta I^*)h\psi}}{(1-h(\psi V^*-(\mu+\epsilon+\gamma)-\alpha))^2} & \frac{\sigma h\beta S^*}{1-h(\psi V^*-(\mu+\epsilon+\gamma)-\alpha)} & 0 & 0 \\ 0 & 0 & \frac{h\alpha}{1+h(\mu+\pi+\omega)} & \frac{1}{1+h(\mu+\pi+\omega)} & 0 \\ 0 & 0 & \frac{h\gamma}{1+h\mu} & \frac{h\omega}{1+h\mu} & \frac{1}{1+h\mu} \end{bmatrix}$$

We consider,

$$K_1 = \frac{1}{1+\frac{h\beta I^*}{\sigma+\eta I^*}+h(\phi+\mu)},$$

$$K_2 = \frac{(h\Lambda+S^*)(2h\eta I^*\beta+\sigma)}{\left(1+\frac{h\beta I^*}{\sigma+\eta I^*}+h(\phi+\mu)\right)^2(\sigma+\eta I^*)^2},$$

$$K_3 = \frac{h\phi}{1+h(\mu+\psi I^*)}, \qquad K_4 = \frac{1}{1+h(\mu+\psi I^*)},$$

$$K_5 = \frac{(h\phi S^*+V^*)(h\psi)}{(1+h(\mu+\psi I^*))^2},$$

$$K_6 = \frac{\frac{h\beta I^*}{\sigma+\eta I^*}}{(1-h(\psi V^*-(\mu+\epsilon+\gamma)-\alpha))},$$

$$K_7 = \frac{\frac{-(1+h\beta S^*)}{(\sigma+\eta I^*)(h\psi)}}{(1-h(\psi V^*-(\mu+\epsilon+\gamma)-\alpha))^2},$$

$$K_8 = \frac{\sigma h\beta S^*}{1-h(\psi V^*-(\mu+\epsilon+\gamma)-\alpha)},$$

$$K_9 = \frac{ha}{1+h(\mu+\pi+\omega)}, \qquad K_{10} = \frac{1}{1+h(\mu+\pi+\omega)},$$

$$K_{11} = \frac{hy}{1+h\mu}, \qquad K_{12} = \frac{h\omega}{1+h\mu}, \qquad K_{13} = \frac{1}{1+h\mu}.$$

Finally,

$$J(E^*) = \begin{bmatrix} K_1 & 0 & K_2 & 0 & 0 \\ K_3 & K_4 & K_5 & 0 & 0 \\ K_6 & K_7 & K_8 & 0 & 0 \\ 0 & 0 & K_9 & K_{10} & 0 \\ 0 & 0 & K_{11} & K_{12} & K_{13} \end{bmatrix}$$

$$|J(E^*) - \lambda I| = 0$$

$$\begin{vmatrix} K_1 - \lambda & 0 & K_2 & 0 & 0 \\ K_3 & K_4 - \lambda & K_5 & 0 & 0 \\ K_6 & K_7 & K_8 - \lambda & 0 & 0 \\ 0 & 0 & K_9 & K_{10} - \lambda & 0 \\ 0 & 0 & K_{11} & K_{12} & K_{13} - \lambda \end{vmatrix} = 0$$

Solve, then we get

$$K_{13} - \lambda = 0$$

$$K_{13} = \lambda$$

$$K_{10} - \lambda = 0$$

$$K_{10} = \lambda$$

$$\begin{vmatrix} K_1 - \lambda & 0 & K_2 \\ K_3 & K_4 - \lambda & K_5 \\ K_6 & K_7 & K_8 - \lambda \end{vmatrix} = 0$$

The characteristic equation for the above equation becomes as

$$-\lambda^3 + \lambda^2(K_1 + K_8 + K_4) - \lambda\left(K_1K_8 + K_1K_4 + K_8K_4 + K_5K_7 - K_2K_6\right) + K_1K_8K_4 + K_1K_5K_7 + K_2K_7K_3 - K_2K_6K_4 = 0.$$

or equivalently,

$$-\lambda^3 + \lambda^2\omega_1 - \lambda\omega_2 - \omega_3 = 0$$

$$\lambda^3 - \lambda^2\omega_1 - \lambda(-\omega_2) - (-\omega_3) = 0. \tag{5}$$

The DEE point the discrete NSFD scheme is LAS whenever $R_0 > 1$, since all solutions to eq (5) must have negative real portions in accordance with the Routh-Hurwitz criterion. □

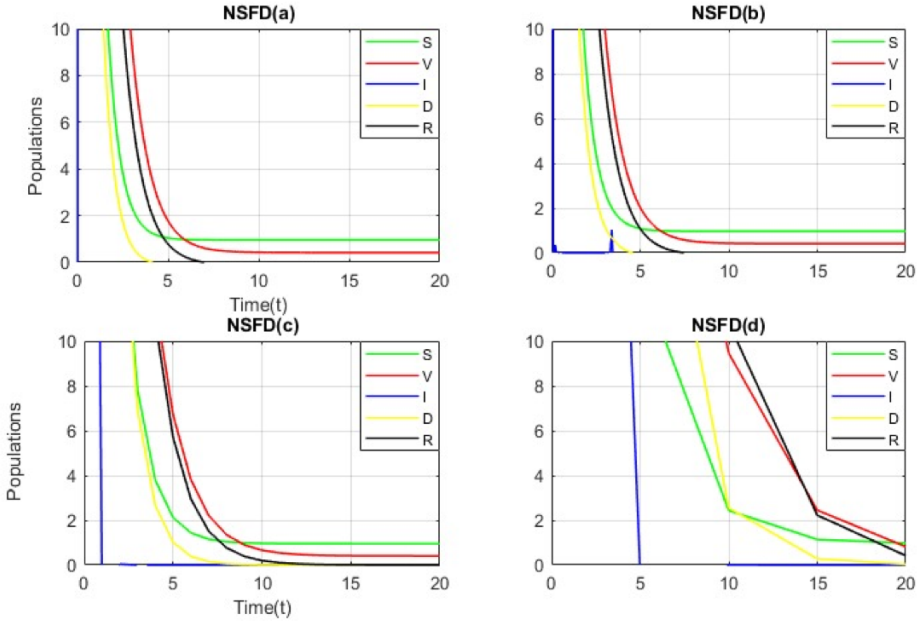

FIGURE 4. Graphs produced by the NSFD

Figure 4. Graphs produced by the NSFD method (a) $h = 0.0001$, (b) $h = 0.001$ (c) $h = 0.01$ and (d) $h = 0.1$. The remaining value of the parameters are offered as $\Lambda = 1.3703, \beta = 0.0108, \psi = 0.01, \phi = 0.43, \gamma = 0.1, \alpha = 0.22, \sigma = 0.22, \epsilon = 0.0271, \eta = 1, \pi = 1, \mu = 1, \omega = 0.2$.

Figure 4 (a-d) illustrates that the NSFD method (7.3) remains stable for each step size. On the other hand, the SFD scheme shows convergence when step sizes are smaller. This exhibit shows that for all step sizes, the NSFD scheme is unconditionally convergent and positive forever.

TABLE 3. Comparison table of step size h

Step size h	**Euler method**	**RK-4 method**	**NSFD method**
0.0001	0.998742	0.998755	0.998756
0.001	0.998610	0.998754	0.998756
0.01	0.997820	0.998742	0.998755
0.1	0.990315	0.998401	0.998752

8. CONCLUSION

The present study develops and analyzes a mathematical describing the transmission dynamics of COVID-19. The qualitative behavior of the epidemic system is examined

through the determination of equilibrium points, namely the DFE and EE. The basic reproduction number is derived as a threshold parameter that determines whether the disease persists or dies out in the population. Stability analysis shows that the DFE is stable when $R_0 < 1$, while the EE exists and becomes stable when $R_0 > 1$, confirming the epidemiological validity of the model. To approximate the solutions, different numerical methods are applied. The classical Euler and RK-4 methods show conditional convergence and strong dependence on step size, which may lead to instability or divergence in long term simulations. In contrast, the NSFD scheme preserve essential qualitative properties such as positivity, boundedness, and stability of solutions independent of step size. The numerical results demonstrate that the NSFD scheme provides more accurate, stable, and dynamically consistent solutions compared to Euler and RK-4 methods. The robustness of the NSFD approach makes it particularly appropriate for epidemiological models where maintaining biological feasibility of solutions is important. The findings of this study contribute to understanding the spread and control of COVID-19 and may assist researchers and public health authorities in predicting disease progression and evaluating intervention strategies. Future research may incorporate additional factors such as vaccination, mutation effects, treatment controls, stochastic perturbations, and fractional-order dynamics to enhance model realism. Overall, the study confirms that the NSFD method is an efficient and reliable numerical technique for solving nonlinear epidemic models and for preserving the structural properties of the original continuous system. Future work may extend the COVID-19 model by incorporating fuzzy parameter membership functions be better represent uncertainty in key parameters including transmission, recovery, vaccination, and treatment rates. The development of fuzzy NSFD schemes may further improve stability and reliability under parameter uncertainty. Additionally, fuzzy sensitivity analysis can help identify influential factors in disease control, and the framework may be adapted to other infectious disease to enhances realistic and robust epidemic modeling under uncertain conditions.

CREDIT AUTHORSHIP CONTRIBUTION'S STATEMENT

Raed Hameed Mahdi, Shah Zeb and Ayesha Kamran: Supervision, Project Management, Methodology, Formal Analysis, Research, Data Curation, Original Draft Writing , funding acquisition, and supervision. Muhammad Rafiq: Formal analysis, methodology, data curation, project administration. Yasir Nawaz, Muhammad Bilal and Muhammad Irfan: Conceptualization, Methodology, Formal Analysis, Research, Data Curation, Original Draft Writing, and Visualization. The final version of the manuscript has been read and approved by all authors.

DECLARATIONS

Conflict of Interest: There are no conflicts of interest, according to the authors

Funding: We want to acknowledge the financial support received from the Universiti Sains Malaysia and Malaysian International Scholarship.

Use of AI Tools Declaration: The writers affirm that this paper was not created using artificial intelligence (AI) methods. However, Quiltbolt and ChatGpt were utilized for rephrasing.

Data Availability: All the data used during this study is accessible within the manuscript.

REFERENCES

[1] N. Ahmed, Z. Wei, D. Baleanu, M. Rafiq and M. A. Rehman, *Spatio-temporal numerical modeling of reaction-diffusion measles epidemic system*, Chaos: An Interdisciplinary Journal of Nonlinear Science. **29**, No.10 (2019): 103101.

[2] R. M. Anderson, C. Fraser, A. C. Ghani, C. A. Donnelly, S. Riley, N. M. Ferguson and A. J. Hedley, *Epidemiology, transmission dynamics and control of SARS: the 2002–2003 epidemic*, Philosophical Transactions of the Royal Society of London. Series B: Biological Sciences. **359**, No.1447 (2004): 1091–1105.

[3] A. A. Anteneh, Y. M. Bazezew and S. Palanisamy, *Mathematical model and analysis on the impact of awareness campaign and asymptomatic human immigrants in the transmission of COVID-19*, BioMed Research International. **2022**, No.1 (2022): 6260262.

[4] F. Avram, R. Adenane, L. Basnarkov, G. Bianchin, D. Goreac and A. Halanay, *An Age of Infection Kernel, an R Formula, and Further Results for Arino–Brauer A, B Matrix Epidemic Models with Varying Populations, Waning Immunity, and Disease and Vaccination Fatalities*, Mathematics. **11**, No.6 (2023): 1307.

[5] A. Ayalew, Y. Molla, T. Tilahun and T. Tesfa, *Mathematical Model and Analysis on the Impacts of Vaccination and Treatment in the Control of the COVID-19 Pandemic with Optimal Control*, Journal of Applied Mathematics. **2023**, (2023): 8570311.

[6] H. Chen, G. J. D. Smith, K. S. Li, J. Wang, X. H. Fan, J. M. Rayner and Y. Guan, *Establishment of multiple sublineages of H5N1 influenza virus in Asia: implications for pandemic control*, Proceedings of the National Academy of Sciences. **103**, No.8 (2006): 2845–2850.

[7] C. Chintu, U. H. Athale and P. S. Patil, *Childhood cancers in Zambia before and after the HIV epidemic*, Archives of Disease in Childhood. **73**, No.2 (1995): 100–105.

[8] N. Chitnis, J. M. Hyman and J. M. Cushing, *Determining important parameters in the spread of malaria through the sensitivity analysis of a mathematical model*, Bulletin of Mathematical Biology. **70**, (2008): 1272–1296.

[9] M. L. Diagne, H. Rwezaura, S. Y. Tchoumi and J. M. Tchuenche, *A mathematical model of COVID-19 with vaccination and treatment*, Computational and Mathematical Methods in Medicine. **2021**, (2021): 1250129.

[10] O. Diekmann, J. A. P. Heesterbeek and J. A. J. Metz, *On the definition and the computation of the basic reproduction ratio R_0 in models for infectious diseases in heterogeneous populations*, Journal of Mathematical Biology. **28**, (1990): 365–382.

[11] B. Fain and H. M. Dobrovolny, *Initial inoculum and the severity of COVID-19: A mathematical modeling study of the dose-response of SARS-CoV-2 infections*, Epidemiologia. **1** No.1, (2020): 5–15.

[12] T. S. Faniran, A. Ali, N. E. Al-Hazmi, J. K. K. Asamoah, T. A. Nofal and M. O. Adewole, *New variant of SARS-CoV-2 dynamics with imperfect vaccine*, Complexity. **2022**, (2022).

[13] A. S. Fauci, *Infectious diseases: considerations for the 21st century*, Clinical Infectious Diseases. **32**, No.5 (2001): 675–685.

[14] S. P. Fisher-Hoch and L. Hutwagner, *Opportunistic candidiasis: an epidemic of the 1980s*, Clinical Infectious Diseases. **21**, No.4 (1995): 897–904.

[15] T. R. Frieden, I. Damon, B. P. Bell, T. Kenyon and S. Nichol, *Ebola 2014—new challenges, new global response and responsibility*, New England Journal of Medicine. **371**, No.13 (2014): 1177–1180.

[16] M. P. Girard, J. S. Tam, O. M. Assossou and M. P. Kieny, *The 2009 A (H1N1) influenza virus pandemic: A review*, Vaccine. **28**, No.31 (2010): 4895–4902.

[17] H. Hamam, Y. Ramzan, S. Niazai, K. A. Gepreel, A. U. Awan, M. Ozair and T. Hussain, *Deciphering the enigma of Lassa virus transmission dynamics and strategies for effective epidemic control through awareness campaigns and rodenticides*, Scientific Reports. **14**, (2024): 18079.

[18] H. S. Hurd and J. B. Kaneene, *The application of simulation models and systems analysis in epidemiology: a review*, Preventive Veterinary Medicine. **15**, No.(2–3) (1993): 81–99.

[19] S. Jain, L. Kamimoto, A. M. Bramley, A. M. Schmitz, S. R. Benoit, J. Louie and L. Finelli, *Hospitalized patients with 2009 H1N1 influenza in the United States, April–June 2009*, New England Journal of Medicine. **361**, No.20 (2009): 1935–1944.

[20] A. Kadri, A. Boudaoui, S. Ullah, M. Asiri, A. B. Saqib and M. B. Riaz, *A comparative study of deterministic and stochastic computational modeling approaches for analyzing and optimizing COVID-19 control*, Scientific Reports. **15**, No.1 (2025): 13755.

[21] C. Kaeuffer, C. Le Hyaric, T. Fabacher, J. Mootien, B. Dervieux, Y. Ruch and COVID Alsace Study Group, *Clinical characteristics and risk factors associated with severe COVID-19: prospective analysis of 1,045 hospitalised cases in North-Eastern France, March 2020*, Eurosurveillance. **25**, No.48 (2020): 2000895.

[22] W. O. Kermack and A. G. McKendrick, *Contributions to the mathematical theory of epidemics. II.—The problem of endemicity*, Proceedings of the Royal Society of London. Series A. **138**, No.834 (1932): 55–83.

[23] M. A. Khan and A. Atangana, *Mathematical modeling and analysis of COVID-19: A study of new variant Omicron*, Physica A: Statistical Mechanics and its Applications. **599**, (2022), 127452.

[24] I. U. Khan, S. Mustafa, A. Shokri, S. Li, A. Akgül and A. Bariq, *The stability analysis of a nonlinear mathematical model for typhoid fever disease*, Scientific Reports. **13**, No.1 (2023): 15284.

[25] A. A. Khan, S. Ullah and R. Amin, *Correction to: Optimal control analysis of COVID-19 vaccine epidemic model: A case study*, The European Physical Journal Plus. **137**, No.2 (2022): 198.

[26] A. M. Kilpatrick, A. A. Chmura, D. W. Gibbons, R. C. Fleischer, P. P. Marra and P. Daszak, *Predicting the global spread of H5N1 avian influenza*, Proceedings of the National Academy of Sciences. **103**, No.51 (2006): 19368–19373.

[27] W. K. Lam, N. S. Zhong and W. C. Tan, *Overview on SARS in Asia and the world*, Respirology. **8**, (2003): S2–S5.

[28] J. D. Lambert, *Numerical Methods for Ordinary Differential Systems: The Initial Value Problem*, John Wiley & Sons, New York. **146**, (1991).

[29] G. E. Lahodny and L. J. Allen, *Probability of a disease outbreak in stochastic multipatch epidemic models*, Bulletin of Mathematical Biology. **75**, (2013): 1157–1180.

[30] D. K. Mamo, *Model the transmission dynamics of COVID-19 propagation with public health intervention*, Results in Applied Mathematics. **7**, (2020): 100123.

[31] R. E. Mickens, *Calculation of denominator functions for nonstandard finite difference schemes for differential equations satisfying a positivity condition*, Numerical Methods for Partial Differential Equations: An International Journal. **23**, No.3 (2007): 672–691.

[32] R. E. Mickens, *Nonstandard finite difference models of differential equations*, World Scientific, Singapore. (1994): 68–92.

[33] M. Naveed, D. Baleanu, M. Rafiq, A. Raza, A. H. Soori and N. Ahmed, *Dynamical behavior and sensitivity analysis of a delayed coronavirus epidemic model*, Computers, Materials & Continua. **65**, No.1 (2020): 225–241.

[34] M. Naveed, M. Rafiq, A. Raza, N. Ahmed, I. Khan, K. Sooppy Nisar and A. Hassan Soori, *Mathematical analysis of novel Coronavirus (2019-nCov) delay pandemic model*, Computers, Materials & Continua. **64**, No.3 (2020): 1401–1414.

[35] R. Nigam, K. Pandya, A. J. Luis, R. Sengupta and M. Kotha, *Positive effects of COVID-19 lockdown on air quality of industrial cities (Ankleshwar and Vapi) of Western India*, Scientific Reports. **11**, No.1 (2021): 4285.

[36] N. Puri, E. A. Coomes, H. Haghbayan and K. Gunaratne, *Social media and vaccine hesitancy: new updates for the era of COVID-19 and globalized infectious diseases*, Human Vaccines & Immunotherapeutics. **16**, No.11 (2020): 2586–2593.

[37] Y. Ramzan, K. Guedri, A. U. Awan, J. Kafle, H. A. Niyazi and B. M. Makhdoum, *Modeling gonorrhea and HIV coinfection with predictive analytics for disability and mortality risks*, Scientific Reports. **15**, (2025): 32983.

[38] Y. Ramzan, B. M. Fadhl, S. Niazai, A. U. Awan and K. Guedri, *Decoding the transmission and subsequent disability risks of rabineurodeficiency syndrome without recuperation*, Scientific Reports. **15**, (2025): 17322.

[39] A. Shokri, M. Mehdizadeh Khalsaraei and M. Molayi, *Nonstandard Dynamically Consistent Numerical Methods for the MSEIR Model*, Journal of Applied and Computational Mechanics. **8**, No.1 (2022): 196–205.

[40] G. Q. Sun, Z. Jin, Q. X. Liu and L. Li, *Chaos induced by breakup of waves in a spatial epidemic model with nonlinear incidence rate*, Journal of Statistical Mechanics: Theory and Experiment. **2008**, No.08 (2008): P08011.

[41] P. Van den Driessche and J. Watmough, *Further notes on the basic reproduction number*, Mathematical Epidemiology. **1945**, (2008): 159–178.

[42] L. Wang, A. A. Khan, S. Ullah, N. Haider, S. A. AlQahtani and A. B. Saqib, *A rigorous theoretical and numerical analysis of a nonlinear reaction–diffusion epidemic model pertaining dynamics of COVID-19*, Scientific Reports. **14**, No.1 (2024): 7902.

[43] Y. Wang, S. Samreen, S. Ullah, I. U. Khan, S. Alqahtani and A. M. Hassan, *Numerical assessment of multiple vaccinations to mitigate the transmission of COVID-19 via a new epidemiological modeling approach*, Results in Physics. **52**, (2023): 106889.

[44] T. Wu, C. Perrings, A. Kinzig, J. P. Collins, B. A. Minteer and P. Daszak, *Economic growth, urbanization, globalization, and the risks of emerging infectious diseases in China: A review*, Ambio. **46**, (2017): 18–29.

[45] H. M. Yang, L. P. Lombardi Junior, F. F. M. Castro and A. C. Yang, *Mathematical modeling of the transmission of SARS-CoV-2—Evaluating the impact of isolation in São Paulo State (Brazil) and lockdown in Spain associated with protective measures on the epidemic of COVID-19*, PLoS ONE. **16**, No.6 (2021): e0252271.

[46] N. Zhu, D. Zhang, W. Wang, X. Li, B. Yang, J. Song and W. Tan, *A novel coronavirus from patients with pneumonia in China, 2019*, New England Journal of Medicine, **382**, No.8 (2020): 727–733.

[47] World Health Organization, *Modes of transmission of virus causing COVID-19: implications for IPC precaution recommendations: scientific brief, 29 March 2020*, WHO/2019-nCoV/Sci_Brief/Transmission_modes/2020.2, 2020.

[48] World Health Organization, *Coronavirus disease 2019 (COVID-19): situation report, 73*, (2020).

[49] WHO Ebola Response Team, *Ebola virus disease in West Africa—the first 9 months of the epidemic and forward projections*, New England Journal of Medicine. **371**, No.16 (2014): 1481–1495.